

Supporting Information

Rational design of aggregation-induced emission sensor based on Rhodamine B for turn-on sensing trivalent metal cations, reversible data protection, and bioimaging

Hai-Xia Yu, Junge Zhi*, Zheng-Feng Chang, Tianjiao Shen, Weilu Ding, Xiaoling Zhang, and Jin-Liang Wang*

Key Laboratory of Cluster Science of Ministry of Education, Beijing Key Laboratory of Photoelectronic/Electrophotonic Conversion Materials, School of Chemistry and Chemical Engineering, Beijing Institute of Technology, Beijing, 100081, P. R. China.

E-mail: jinlwang@bit.edu.cn; jungezhi@bit.edu.cn

Contents

Fig. S1 ^1H NMR spectrum (in CDCl_3) of **TPEThRB**.

Fig. S2 ^{13}C NMR spectrum (in CDCl_3) of **TPEThRB**.

Fig. S3 Mass spectrum (ESI) of **TPEThRB**.

Fig. S4 Absorption spectra of **TPEThRB** ($10 \mu\text{M}$) in $\text{CH}_3\text{CN}-\text{H}_2\text{O}$ mixtures ($f_w = 0\text{-}99\%$).

Fig. S5 Particle size distributions of **TPEThRB** in $\text{CH}_3\text{CN}-\text{H}_2\text{O}$ mixtures with different water contents, (a) $f_w = 60\%$, (b) $f_w = 70\%$, (c) $f_w = 80\%$ and (d) $f_w = 90\%$.

Fig. S6 The 2D stacking modes of **TPEThRB** along (a) a axis, (b) b axis and (c) 3D stacking mode.

Fig. S7 Response time of **TPEThRB** ($10 \mu\text{M}$) in $\text{CH}_3\text{CN}-\text{H}_2\text{O}$ (v:v 3:2) mixtures with Fe^{3+} ($50 \mu\text{M}$), Al^{3+} ($150 \mu\text{M}$), Cr^{3+} ($150 \mu\text{M}$), H^+ ($150 \mu\text{M}$).

Fig. S8 Fluorescence titration plots of compound **TPEThRB** ($10 \mu\text{M}$) in $\text{CH}_3\text{CN}-\text{H}_2\text{O}$ solution with different species (a) Fe^{3+} , (b) Al^{3+} , (c) Cr^{3+} , (d) H^+ .

Fig. S9 The plots of $[\text{I}'/\text{I}_0 - 1]$ versus the concentration of trivalent metal cations and H^+ , (a) Fe^{3+} , (b) Al^{3+} , (c) Cr^{3+} , (d) H^+ .

Fig. S10 UV-vis absorption spectra of **TPEThRB** with monovalent and divalent metal ions.

Fig. S11 Fluorescence spectra of compound **TPEThRB** with different species (a) Fe^{3+} , (b) Al^{3+} , (c) Cr^{3+} in $\text{CH}_3\text{CN-PBS}$ (10 mM , $\text{pH} = 7.4$) mixture.

Fig. S12 ^1H NMR spectra (in CDCl_3) of (a) **TPEThRB**, (b) **TPEThRB** with H^+ ion and (c) compound **1**

Fig. S13 Molecular orbitals of **TPEThRB** through DFT calculations with the B3LYP method.

Fig. S14 The photographs of blank filter paper exposed to TFA vapor under natural light and the 365 nm UV lamp illumination.

Fig. S15 Normalized Fluorescence spectra of **TPEThRB** in the absence and presence of Fe^{3+} , Al^{3+} and Cr^{3+} ions.

Table S1 The summarizing list of detection limits of materials for sensing Fe^{3+} , Al^{3+} and Cr^{3+} ions.

Table S2 CheckCIF report of XRD data of single crystal of **TPEThRB** (CCDC 1814395).

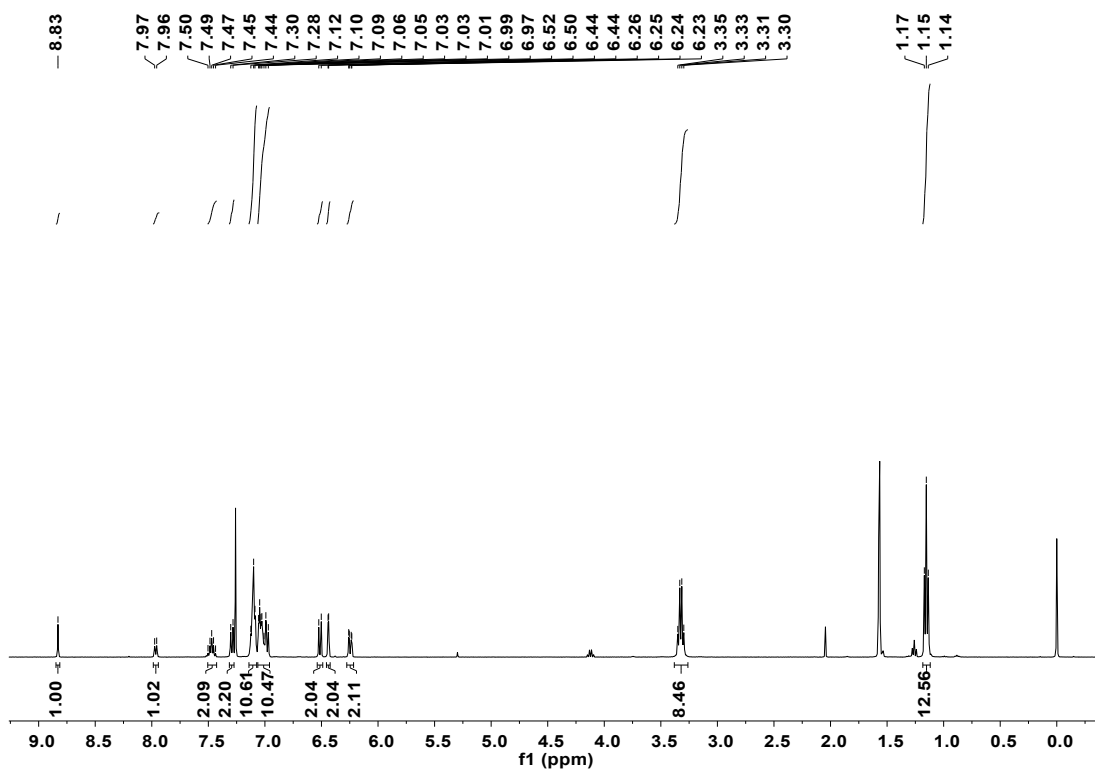


Fig. S1 ^1H NMR spectrum (in CDCl_3) of TPETHRB.

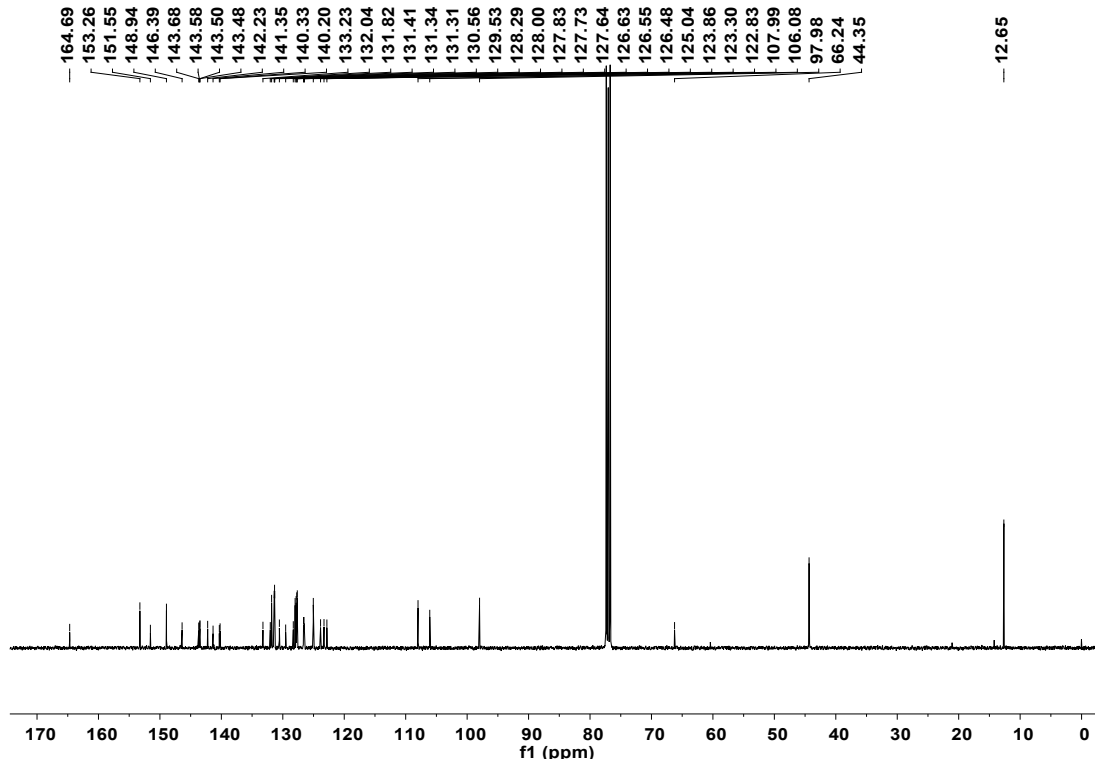


Fig. S2 ^{13}C NMR spectrum (in CDCl_3) of **TPEThRB**.

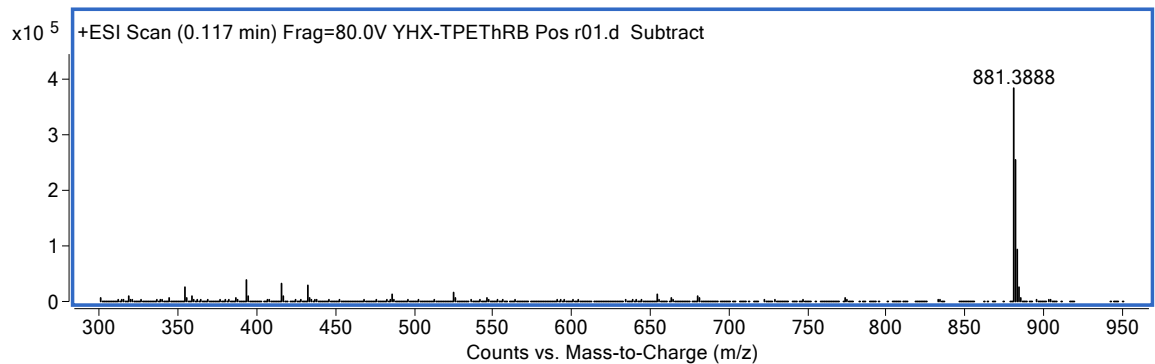


Fig. S3 Mass spectrum (ESI) of TPEThRB.

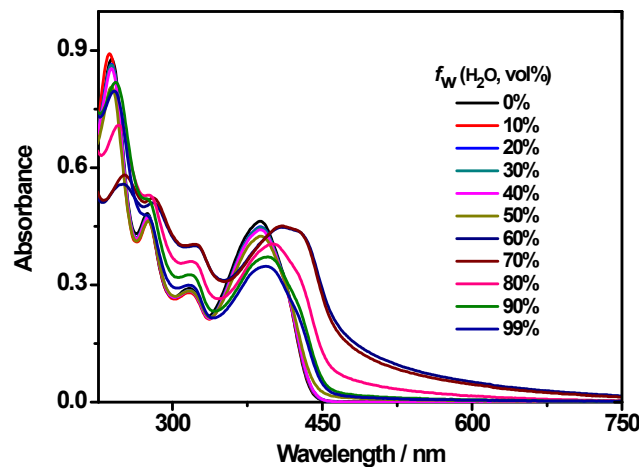


Fig. S4 Absorption spectra of TPEThRB (10 μM) in $\text{CH}_3\text{CN}-\text{H}_2\text{O}$ mixtures ($f_w = 0\text{-}99\%$).

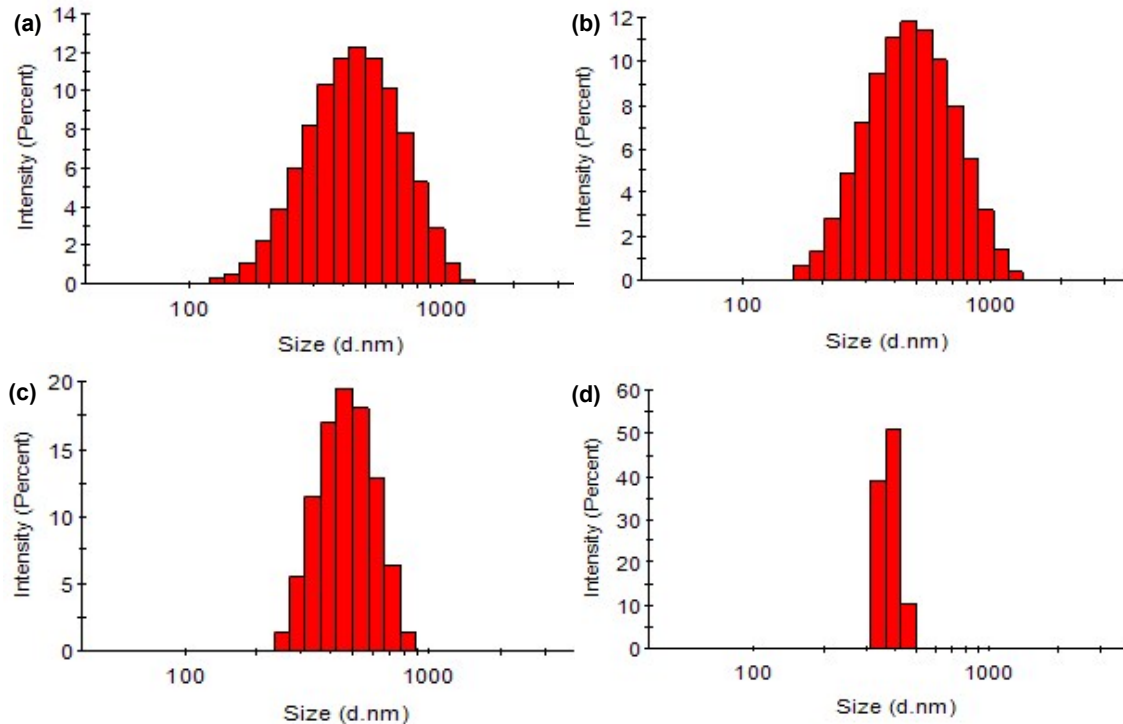


Fig. S5 Particle size distributions of TPEThRB in $\text{CH}_3\text{CN}-\text{H}_2\text{O}$ mixtures with different water contents, (a) $f_w = 60\%$, (b) $f_w = 70\%$, (c) $f_w = 80\%$ and (d) $f_w = 90\%$.

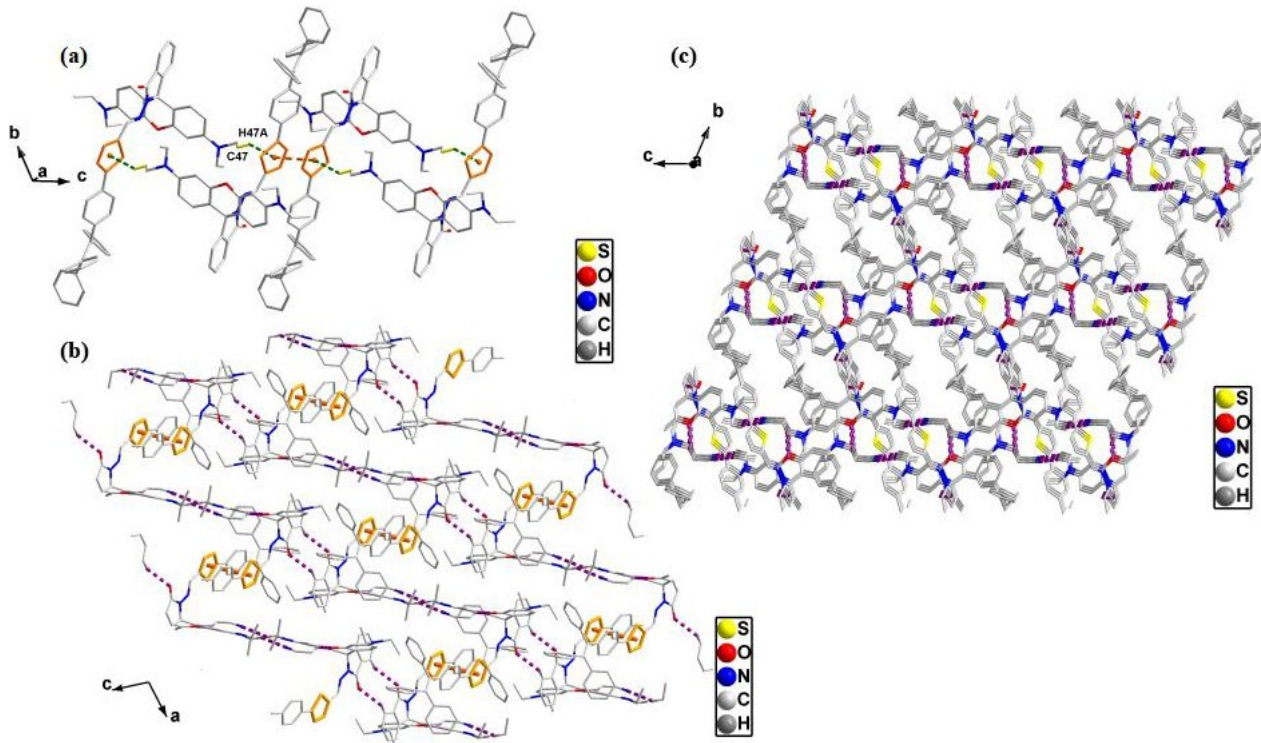


Fig. S6 The 2D stacking modes of **TPEThRB** along (a) **a** axis, (b) **b** axis and (c) 3D stacking mode.

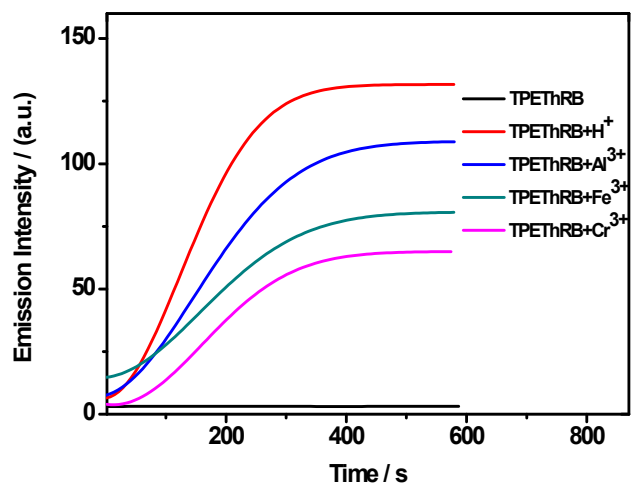


Fig. S7 Response time of **TPEThRB** (10 μ M) in CH₃CN-H₂O (v:v 3:2) mixtures with Fe³⁺ (50 μ M), Al³⁺ (150 μ M), Cr³⁺ (150 μ M), H⁺ (150 μ M).

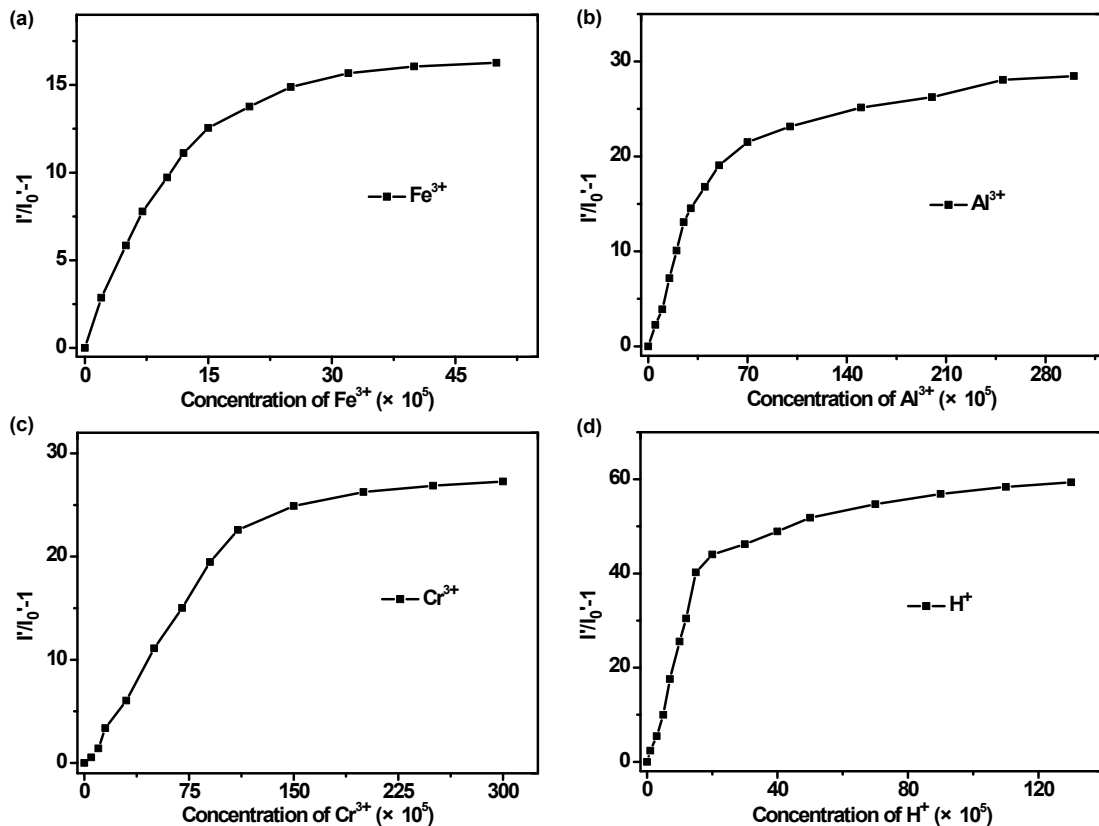


Fig. S8. Fluorescence titration plots of compound **TPEThRB** (10 μM) in $\text{CH}_3\text{CN}-\text{H}_2\text{O}$ solution with different species (a) Fe^{3+} , (b) Al^{3+} , (c) Cr^{3+} , (d) H^+ .

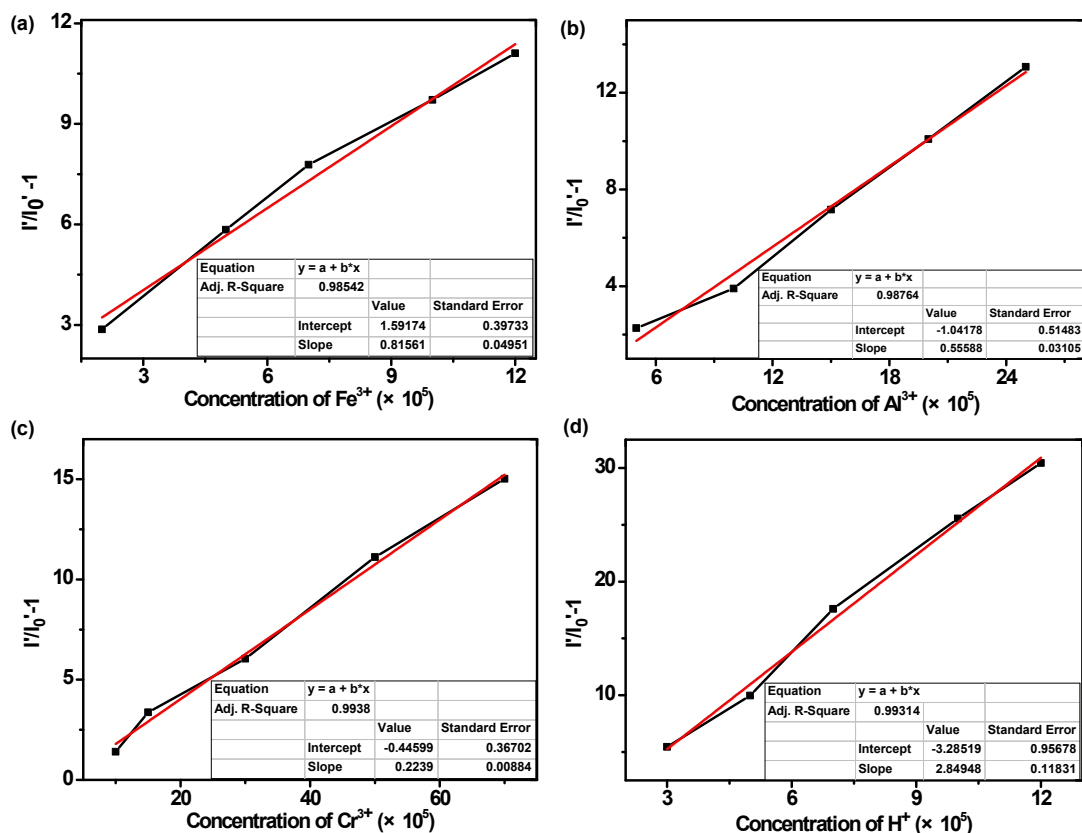


Fig. S9 The plots of $[I'/I_0'^{-1}]$ versus the concentration of trivalent metal cations and H^+ , (a) Fe^{3+} , (b) Al^{3+} , (c) Cr^{3+} , (d) H^+ .

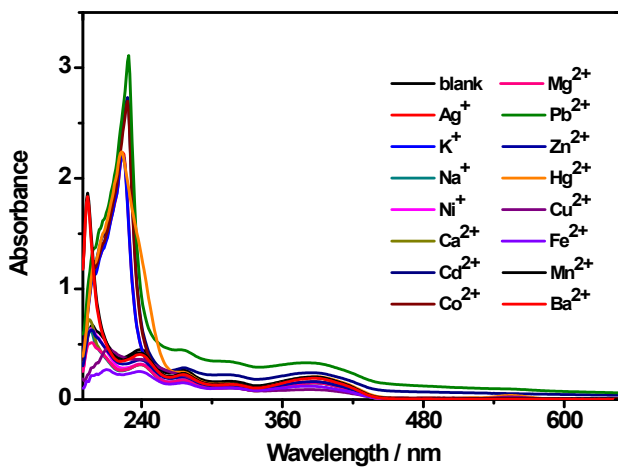


Fig. S10 UV-vis absorption spectra of TPEThRB with monovalent and divalent metal ions.

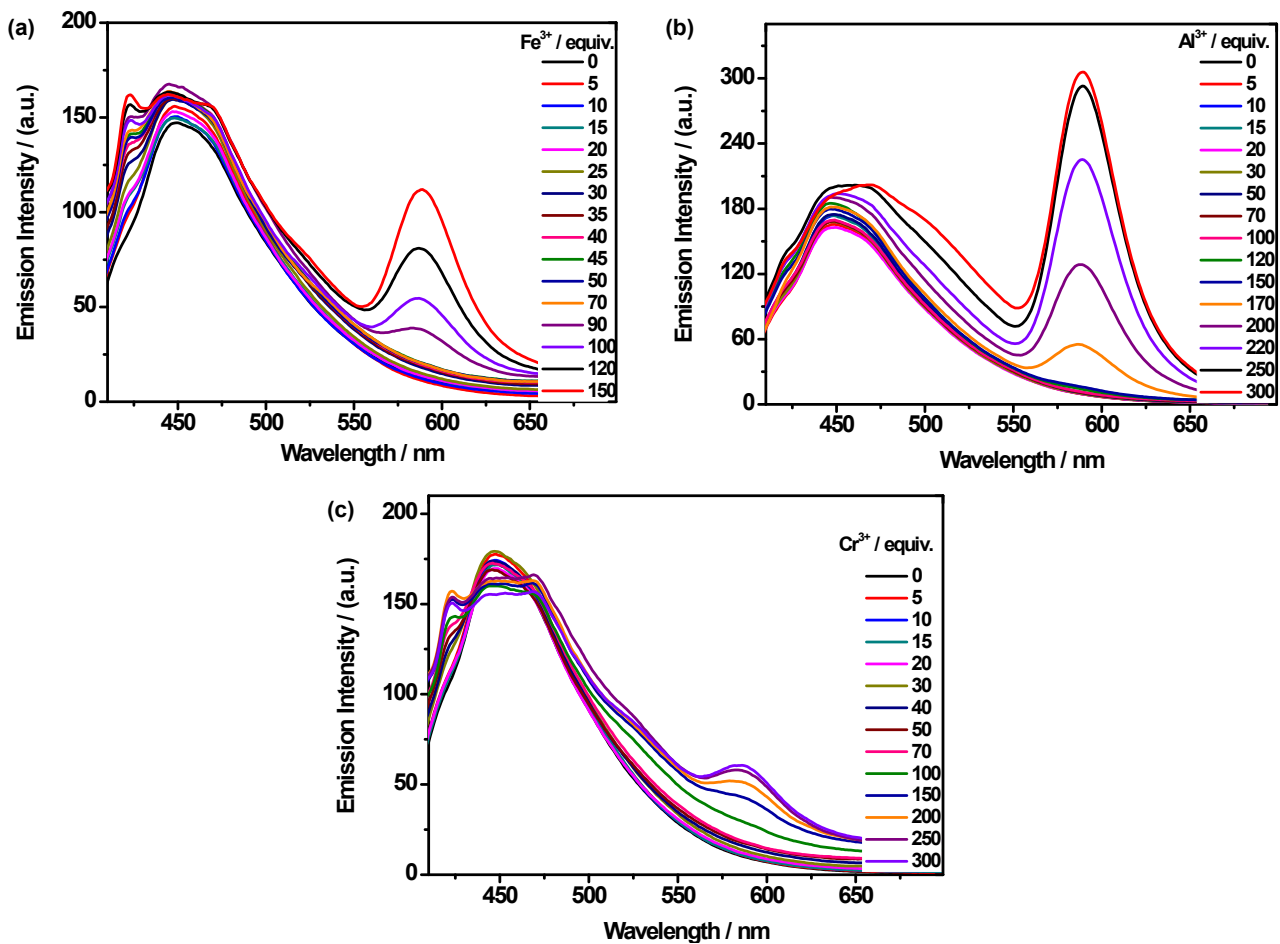


Fig. S11 Fluorescence spectra of compound TPEThRB with different species (a) Fe^{3+} , (b) Al^{3+} , (c) Cr^{3+} in CH_3CN -PBS (10 mM, pH = 7.4) mixture.

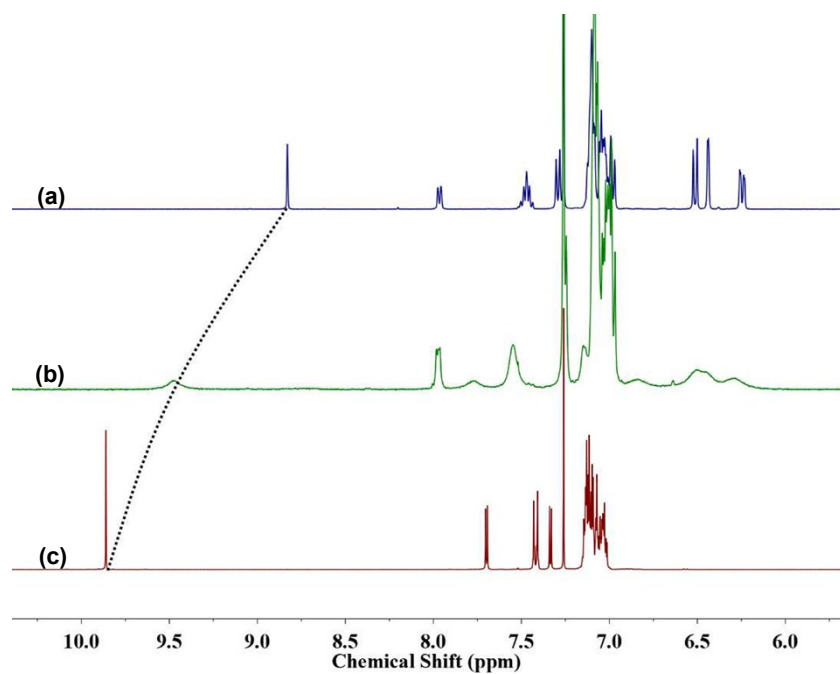


Fig. S12 ¹H NMR spectra (in CDCl₃) of (a) TPEThRB, (b) TPEThRB with H⁺ ion and (c) compound 1.

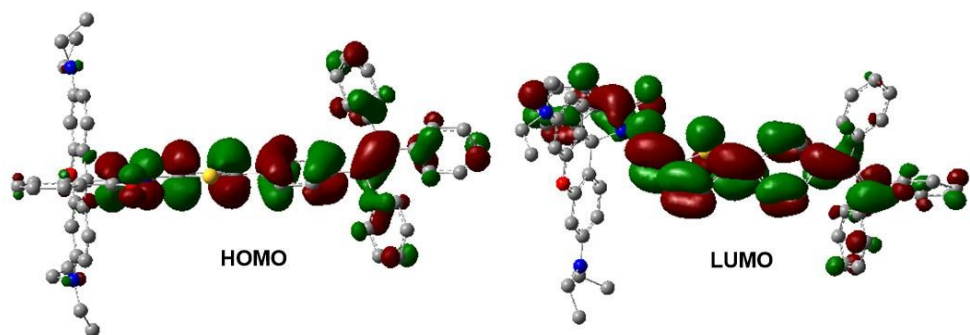


Fig. S13 Molecular orbitals of TPEThRB through DFT calculations with the B3LYP method.

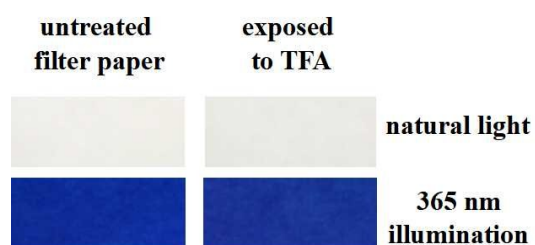


Fig. S14 The photographs of blank filter paper exposed to TFA vapor under natural light and the 365 nm UV lamp illumination.

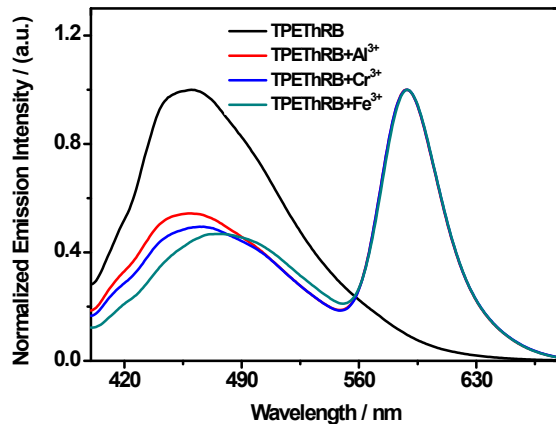


Fig. S15 Normalized fluorescence spectra of TPEThRB in the absence and presence of Fe^{3+} , Al^{3+} and Cr^{3+} ions.

Table S1 The summarizing list of detection limits of materials for sensing Fe^{3+} , Al^{3+} and Cr^{3+} ions.

Material	LOD of Fe^{3+} (μM)	Material	LOD of Al^{3+} (μM)	Material	LOD of Cr^{3+} (μM)
bis(rhodamine)	50	6-thoxychromone-3-carbaldehyde-hydrazone	0.18	Pyrene derivative PB	0.23
Phenanthroimidazole derivative	5.26	napthalimide and naphthaldehyde-based derivative	6.28	rhodamine-2-amino-5-bromopyrimidine	4.9
salicylaldehydeazine	9.5	Eu-BTB anionic framework	100	$\{[\text{Zn}_2(\mu_3-\text{OH})(\text{cpt})](4,4'\text{-bipy})]\cdot\text{H}_2\text{O}\}_n$	5.55
Zn-MOF-74 nanodot	1.04	naphthalene-quinoline derivative	0.0367	2,7-disubstituted phenanthrene derivative	400
2D terbium(III) coordination polymer Tb-CP	0.05	copolymer-ATP supramolecular complex CP-ATP	3.7	Rhodamine capped gold nanoparticles	9.28
TPEThRB	3.2	TPEThRB	4.8	TPEThRB	11.9

Table S2 CheckCIF report of XRD data of single crystal of **TPEThRB** (CCDC 1814395).

Bond precision:	C-C = 0.0049 Å	Wavelength=0.71073	
Cell:	a=13.5619(9) alpha=110.309(2)	b=13.7951(10) beta=101.188(2)	c=15.3779(11) gamma=97.849(2)
Temperature:	296 K		
	Calculated	Reported	
Volume	2581.1(3)	2581.1(3)	
Space group	P -1	P -1	
Hall group	-P 1	-P 1	
Moiety formula	C ₅₉ H ₅₂ N ₄ O ₂ S, C ₂ H ₃ N		
Sum formula	C ₆₁ H ₅₅ N ₅ O ₂ S	C ₆₁ H ₅₅ N ₅ O ₂ S	
Mr	922.16	922.16	
Dx,g cm ⁻³	1.186	1.187	
Z	2	2	
Mu (mm ⁻¹)	0.111	0.111	
F000	976.0	976.0	
F000'	976.60		
h,k,lmax	16,16,18	16,16,18	
Nref	9147	9139	
Tmin,Tmax	0.982,0.989	0.980,0.989	
Tmin'	0.980		
Data completeness=	0.999	Theta(max)= 25.048	
R(reflections)=	0.0572(5281)	wR2(reflections)= 0.1466 (9139)	
S =	1.019	Npar = 622	